Proceedings of Iran International Aluminum Conference (IIAC2016)
May 11-12, 2016, Tehran, I.R. Iran

Experimental Study and Characterization of Activated Alumina Adsorbent

Shahriar Azarfar [a], Farshid Noorbakhsh [b], Mahdi Salmani [c], Sara Ansari [c], Rana Soleymani [a], Sepehr Sadighi [d]
[a] *Nitel Pars Co. (Fateh Group), R&D Department, No. 32, Aftab St., Khodami St., Vanak Sq., P.C. 1994983115 Tehran, Iran.*
[b] *Nitel Pars Co. (Fateh Group), Managing Director, No. 32, Aftab St., Khodami St., Vanak Sq., P.C. 1994983115 Tehran, Iran.*
[c] *Nitel Pars Co. (Fateh Group), Laboratory Disc., Nitel Pars Production Complex, Shiraz Special Economic Zone, P.C. 1994964743 Shiraz, Iran*
[d] *Research Institute of Petroleum Industry (RIPI), Catalysis Research Division, West Blvd. Azadi Sport Complex, P.O. Box 14665-137, Tehran, Iran*

Abstract: This paper is devoted to specify properties of activated alumina, determine its adsorption characteristics, and calculate its adsorption rates as a significant parameter for designing adsorption process. In this regard, the most physical properties such as crush strength and particle size distribution of adsorbent were determined using modern and advanced devices. The Brunauer–Emmett–Teller (BET) test was carried out to determine the specific surface area, pore diameter and pore volume of the activated alumina which were 334.67 m^2/g, 8.096 nm, and 0.0713 cm^3/g, respectively. Additionally, chemical and morphological specifications such as pore size distribution of adsorbents assess textural properties of the activated alumina were characterized using X-ray fluorescence (XRF) and Barrett-Joyner-Halenda (BJH) analysis, respectively. Also, adsorption isotherm of the activated alumina were determined using Langmuir, Freundlich and BET models.

Keywords: Activated Alumina; Physical Characterization; Adsorption

1. Introduction

Activated alumina is a type of aluminum oxide which is manufactured from aluminium hydroxide by dehydroxylating. A highly porous material with a surface area of higher than 200 m^2/g can be produced by this reaction. It is obvious that a material with this feature can be applied as a support material for a broad spectrum of catalytic and adsorption applications**.** Several outstanding studies are known as the root of alumina knowledge through the 1970's due to their valuable researches and studies about structures and textures of alumina. In this context, it can be mentioned authors such as Stumpf et al. [1], Lippens [2], Gitzen [3], and Wefers [4] that illustrate the importance of this material. It has also been proved that alumina have many technological and industrial applications due to its various crystallographic modifications which α-, γ-, δ- and θ- polymorphs are the most important. α-alumina is a very inert and hard material, whereas γ- and δ- alumina are widely used catalysts, not only as supports but also as typical acid-base catalyst [5]. On the other hand, the θ-alumina structure can be described as a distorted cubic closest-packed array of oxygen anions in which the aluminum cations occupy one-eighth of the tetrahedral interstices and half of the octahedral ones [6]. The term alumina generally covers four classes of aluminium compounds [7]:

1. Aluminium trihydroxides with the formula $Al(OH)_3$: γ-$Al(OH)_3$ (gibbsite), α- $Al(OH)_3$ (bayerite). 2. Aluminium oxides with the formula AlOOH (bayerite). -γ-AlOOH boehmite (highly crystalline, crystalline, fibrillar) with face-centered cubic close-packed oxygen sublattice, α-AlOOH (diaspore) with hexagonal close-packed oxygen sublattice, 3. Transition alumina is high surface area oxides derived from $Al(OH)_3$ or AlOOH;

4. α-$A1_2O_3$ (or corundum) is the thermodynamically stable phase of aluminium oxide with hexagonal close-packed oxygen sublattice.

Investigation on additional forms of alumina are beyond the scope of this study, which is devoted to characterization of activated alumina as adsorbent. Therefore, among others, γ-alumina is only intended because it has a high surface area and is relatively stable over the temperature range of interest for most catalytic reactions and adsorption processes. The γ-alumina is widely used in adsorption industry, especially as a support in heterogeneous catalysis [8-10], due to its low cost and textural properties [11-13]. In terms of chemical, γ-alumina is unique material which its chemical properties are closely related to the hydroxyl (OH) groups i.e., the coexistence of OH groups and coordinated unsaturated (CUS) Lewis acid sites on the surfaces makes it a bi-functional support. This feature leads to γ-alumina being able to graft chemical species with the OH groups, and be open to be attacked by nucleophiles at the CUS concurrently [14]. Therefore, it is expected that γ-alumina to be able to provide additional catalytic functions to the active phase when it is used as a support. Despite these characteristics and features, the synthesis of alumina with hierarchically ordered pore structure attracts more and more attention, due to the highly effective transport phenomena, and the easy diffusion of reactants and products when pores of different sizes are interconnected [15]. Generation of controllable hierarchical pores has been fundamentally carried out through agents acting as porosity generators like organic additives and surfactants [16, 17], foams, emulsions or masks based on replica procedure [18], as well as by using others methods as hydrothermal treatment [19], and recently, nano-casting technique [20].

*Corresponding author: Tel.: +98-21-88604147 Fax: +98-21-88604158
E-mail address: R&D002@NitelPars.com.

Over some decades researchers have investigated and explored several methods of porous alumina synthesis with high surface area and varied pore structures to prepare activated alumina that being able to adsorb various material as desiccator based on its pore structure. Monica Benitez-Guerrero and co-workers synthesized mesoporous γ-alumina fibers with BET surface area of 200 m^2/g using the replica method of sisal fibers as templates. They determined specific surface area and porosity of ceramic fibers by N_2 and CO_2 adsorption-desorption measurements. The obtained results indicated alumina fibers retained high specific surface areas of 200 m^2/g and 150 m^2/g even after calcination at 1000°C for 15 h in dry air and for 4 h in wet air, respectively [15]. Shiau and Fang [21] provided α-alumina using citrate process with α-alumina seeding. They were found that the transformation temperature of α-alumina could be lowered to 900℃. Qingling Wu et al. [17] synthesized alumina via one-step process using aluminum iso-propoxide as an inorganic precursor, pluronic P123 as a template, hydrochloric acid and citric acid as the pH adjustors, and 1,3,5-trimethylbenzene (TMB) as a swelling agent. They also reported that mesoporous aluminas have relatively high surface areas (up to 309 m^2/g), pore volumes (0.51 cm^3/g), large pore sizes (up to 7.5 nm), and high thermal stability (up to 900℃). In addition, they demonstrate the weight ratios of TMB/P123 play an important role in the synthesis process for controlling the mesostructures and pore sizes of the materials. On the other hand, production of alumina from natural minerals has attracted much attention of researchers. So that, organic–inorganic assemblies involving complicated sol–gel processes by using surfactants as structure-directing agents are regarded as the most promising approaches. They includes synthesis of alumina from boehmite [22] and gibbsite [23].

The main objective of this paper is investigation and characterization of the physical properties of activated alumina e.g., surface area, pore volume, adsorption capacity, Barrett-Joyner-Halenda (BJH) analysis etc. which are key elements to understand and control the use of this material in adsorption processes particularly. In this work, it is also aimed to enlarge the necessity of surface alumina modification using appropriate materials to make alumina more compatible with desired media.

2. Experimental Procedure

2.1. Materials

Commercial activated alumina and other employed materials in this work were supplied by Nitel Pars Company, Iran. The purified nitrogen (99%) gas was also used to determine surface area and porosity of sample.

2.2. Synthesis of activated alumina

Fig. 1 shows the flow chart of the processes employed in NitelPars laboratory for synthesizing activated alumina from a type of binder like kaolin as reported in the literatures [5, 16, 17, 22, 24]. In general, the binder is firstly de-aluminated to produce aluminum sulfate. Aluminum hydroxide is precipitated from the aluminum sulfate according to Eq. (1). The aluminum hydroxide precipitated is then calcined to produce activated alumina according to Eq. (2) [24]. Hereafter, the activated alumina formed is referred to as HYAA300 in the subsequent discussion.

$$Al_2(SO_4)_3 + 6NaOH \rightarrow 2Al(OH)_3 + 3Na_2SO_4 \quad (1)$$

$$2Al(OH)_3 \rightarrow Al_2O_3 + 3H_2O \quad (2)$$

2.3. Adsorption study

Adsorption study of HYAA300 was carried out by TriStar Micromeritics device (see Fig. 2) to determine the surface area and porosity of the activated alumina in N_2 adsorption process. The Micromeritics TriStar II 3020 use nitrogen, argon, carbon dioxide, or other non-corrosive gases such as butane, methane, etc. to characterize the micropores below 10 angstroms [25]. TriStar II 3020 is an automated gas adsorption analyzer with three ports allowing up to three samples to be analyzed simultaneously. In this work, sample was firstly degassed at 400℃ for 2 h measurement of equilibrium pressure of a known volume of liquid nitrogen for generation of adsorption–desorption isotherms. Barrett–Joyner–Halenda (BJH) and t-plot method were used to evaluate the average pore size distribution cum total pore volume, respectively while the

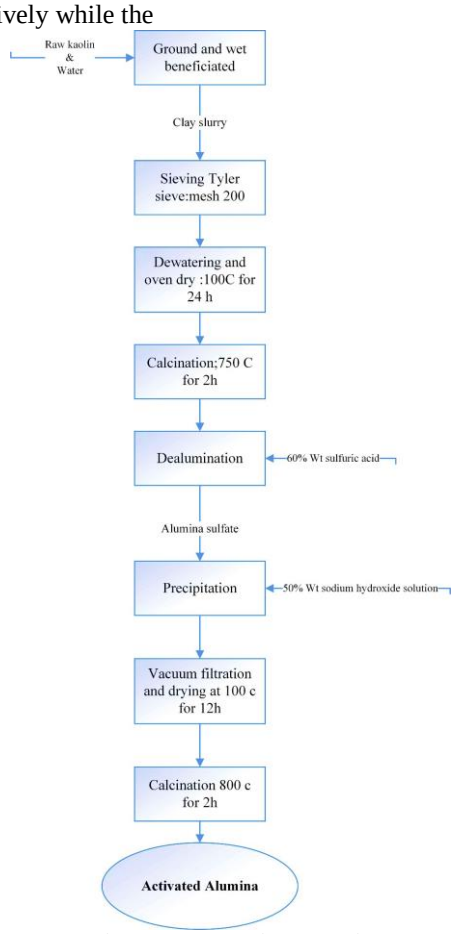

Figure 1. Flow chart for the synthesis of activated from a type of binder.

BET equation was used to calculate the surface area. It is noteworthy that the BJH technique characterises pore size distribution independent of external area due to particle size of the sample.

2.4. Characterization techniques

Certain physical properties of adsorbents are involved in all adsorption design calculations. Therefore, to achieve the best design for adsorption processes, the most important physical properties must be determined because they can virtually never be predicted. The necessary properties are crush strength, dry attrition, surface area and porosity, loss on ignition, and water adsorption.

In this regard, a test sample of 50 to 200 individual pieces of activated alumina were randomly selected to measure the crush strength according to the ASTM D4179 procedure. As seen in Fig. 3a, between 800 and 1000 mL of the test specimen were carefully poured into the tared graduated cylinder using a funnel for tapped density measuring of the HYAA300. For particle size determining, the samples were placed on the top sieve (largest on top), and then sieving continued for 2 min after no further separation was detectable (see Fig. 3b).

Figure 2. Image of TriStar Micromeritics device.

(a) (b)

Figure 3. Tapped bulk density device (a) and sieve analysis device (b).

X-ray fluorescence (XRF) analysis was carried out using ARL™ PERFORM'X device. As already mentioned, BET and BJH analysis was carried out using Tristar II 3020 device. It should be noted that all measurements were carried out according to the ASTM standard test methods in NitelPars Co. laboratory.

3. Results and Discussions

It is clear that HYAA300 destined for use as adsorbents must not only have a good adsorptive capacity, but also excellent mechanical properties, in particular a good resistance of crushing. In this regard, Fig. 4a shows obtained results for crush strength of 100 individual particles which are selected randomly. It is appreciated that the mean value of crush resistance obtained (132.4 N) is with respect to activated alumina having a mean diameter ranging from 3.15 to 6.3 mm (average 4.49mm). Also, the frequency distribution (bell curve) of obtained data showed that crush strength results are balancing – creating a normal distribution pattern. As shown in Fig. 4b, more crush strength results (up to 68%) are between 90 to 190N that shows activated alumina has very high resistance to crushing. This is a result of the production process and the spherical shape of the beads. The attrition and crushing values for spheres are well adapted to their applications. In this work, the supplied activated alumina had spherical form that made possible homogeneous and compact loading with very little subsequent settling.

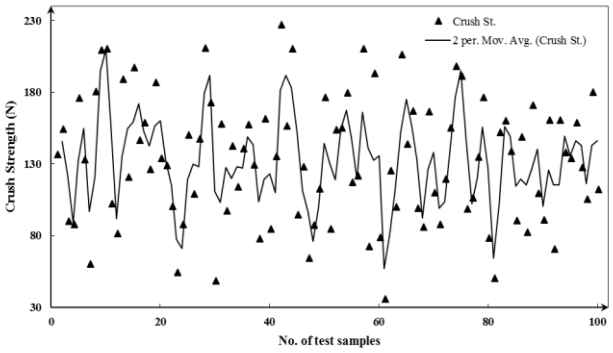

(a)

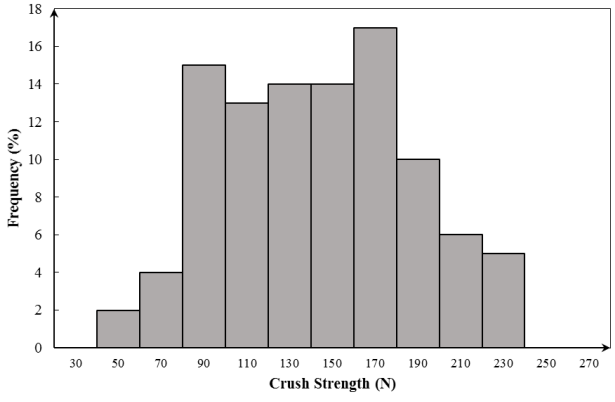

(b)

Figure 4. Crush strength results for 100 individual samples of HYAA300 (a), frequency distribution (bell curve) of results (b).

The elemental and chemical analysis of the activated alumina is presented in Table 1. X-ray fluorescence result evidenced that the HYAA300 has strong crystalline structure due to presence of γ-alumina more than 96.5 wt.%. Meanwhile, it should be pointed out that the percentage of Fe oxide can be more decreased by acid activation, suggesting possible transformation of minerals containing Fe element. Thus, the cleaning of effective adsorption sites on the surface and decrease of the mineralogical inhomogeneity and intensity of activated alumina resulted in a higher BET surface area and total pore volume. Adsorption isotherms are critical to evaluate the sorption capacity of adsorbents as well as to understand the nature of adsorbate–adsorbent interactions. The adsorption isotherms of N_2 gas onto HYAA300 was examined. The experiment was conducted at temperature value of -195.85℃. Three commonly used models, the Langmuir [26], Freundlich [27] and Brunauer-Emmett-Teller (BET) [28] equations were employed to correlate the experimental data, which can be expressed as following equations, respectively.

$$\frac{q}{q_m} = \frac{BC_e}{1+BC_e} \quad (3)$$

$$q = k_f C_e^{1/n} \quad (4)$$

$$\frac{1}{q(1/C_e - 1)} = \frac{c_f - 1}{q_m c_f} C_e + \frac{1}{q_m c_f} \quad (5)$$

Where q (mmol/g) is the amount of N_2 adsorbed at equilibrium; q_m (mmol/g) is the maximum N_2 adsorption capacity; B (L/mmol) is the Langmuir constant that is related to the apparent energy of adsorption; k_f (mmol/g(L/mmol)$^{1/n}$) is the Freundlich constant indicating the relative adsorption capacity, and n is a constant depicting the sorption intensity; c_f is BET dimensionless constant that is related to the enthalpy of adsorption of the adsorbate gas on sample. The Langmuir equation is derived from the assumption of monolayer adsorption on specific homogenous sites, while the Freundlich model represents adsorption on heterogeneous surfaces. The concept of BET model is an extension of Langmuir theory to multilayer adsorption with the following hypotheses: (a) gas molecules physically adsorb on a solid in layers infinitely; (b) there is no interaction between each adsorption layer; and (c) the Langmuir theory can be applied to each layer [28].

As shown in Fig. 5, the Langmuir, Freundlich and BET models correlated the sorption isotherms on HYAA300. But, the BET model was fitted quite well with R-value higher than 0.99, compared to others. As-fitted Langmuir, Freundlich and BET parameters for the adsorption of N_2 onto HYAA300 are listed in Table 2. The good application of BET model implied that besides adsorption onto specific sorption sites through chemical interactions such as surface complexation and cation bridging, adsorbate–adsorbate interaction may also play an important role in the sorption process. Fig 5c confirms that the BET model must be selected as adsorption isotherm correlation for predicting the adsorption capacity of the HYAA300. The surface area and molecular cross-sectional area of HYAA300 were determined 334.6737 m^2/g and 0.162 nm^2, respectively.

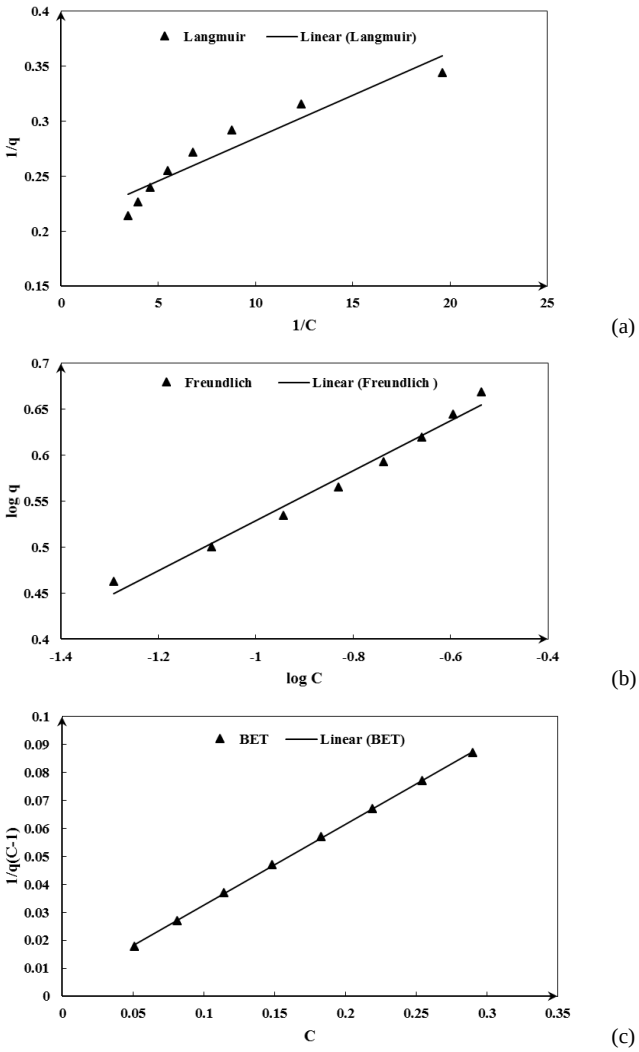

Figure 5. Curve fitting of experimental data using Langmuir (a); Freundlich (b) and BET (c) models.

Table 1. X-ray fluorescence result for HYAA300.

Composition	Value (wt.%)
γ-Al_2O_3	96.7
Fe_2O_3	0.04
L.O.I[a]	3.26

[a] To determine the mass loss, sample was heated for 1 hr. at 900℃. The mass loss can be due to the loss of moisture, carbon, sulfur, and so forth, from the decomposition or combustion of the residue.

Table 2. Langmuir and Freundlich isotherm parameters for adsorption of N_2 on activated alumina.

parameters	Langmuir	Freundlich	BET
q_m (mmol/g)	4.8355	----	3.43047
B, k_f or c_f	26.5128	6.332	64.5398
n	----	3.667	----
R^2	0.9032	0.9808	0.9998

The adsorption and desorption isotherms of nitrogen gas on HYAA300 are presented in Fig. 6. According to the IUPAC classification, the adsorption isotherm infer to sorption in mesoporous (pore size is generally 2-50 nm) with strong affinities. In this case, capillary condensation occurs in the pores. Also, from comparison hysteresis loops in this figure with IUPAC deduced that mesopore geometries are tubular capillary open at both ends, tubular capillaries with various forms of cross sections that can be investigated by appropriate tests such as Scanning Electron Microscope (SEM) in future works. The mesoporous is good model for HYAA300 because of its narrow pore size distribution. The BJH pore size distributions for adsorption and desorption have been shown in Fig. 7 and Fig. 8, respectively. It can see clearly that HYAA300 has the pore size distribution in the mesoporous range (1–10 nm).

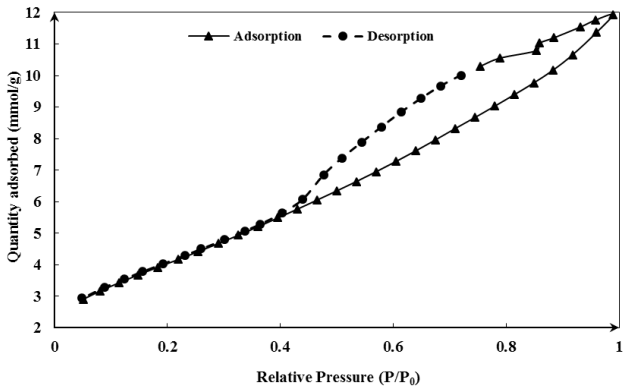

Figure 6. Adsorption and desorption isotherm of N_2 on HYAA300 (P_0 refers to standard pressure, 101.325 kPa).

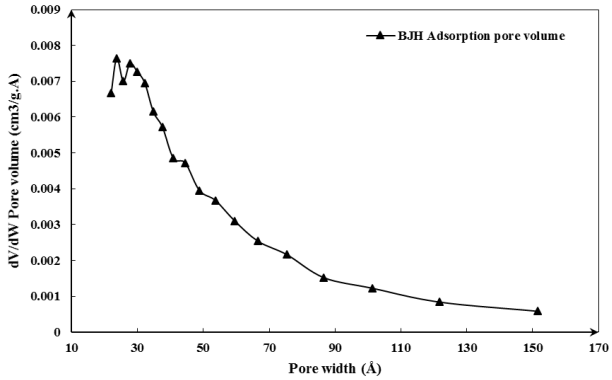

a)

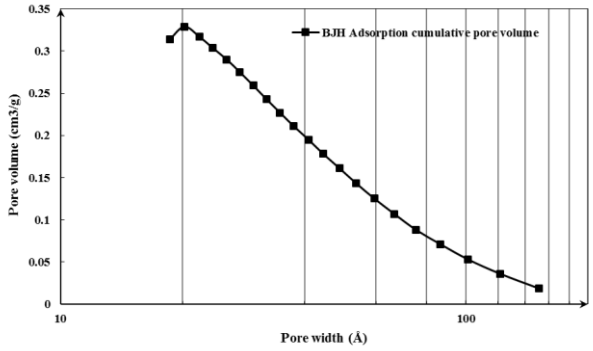

b)

Figure 7. Pore size distribution of HYAA300 (adsorption).

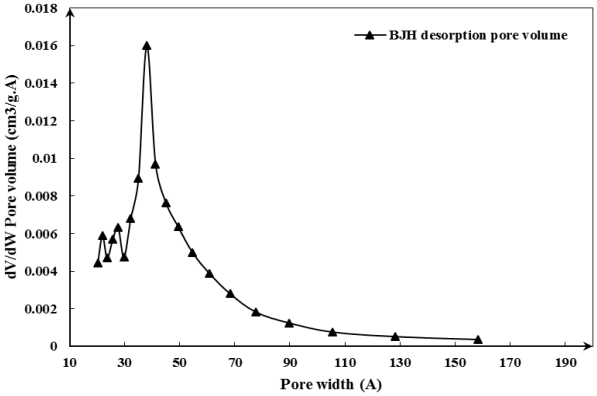

(a)

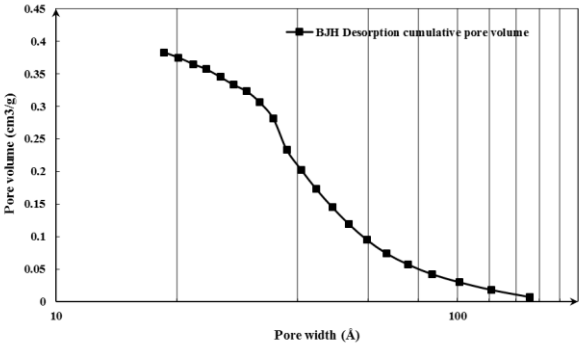

(b)

Figure 8. Pore size distribution of HYAA300 (desorption).

It is estimated from the peaks that mesopores are about 3–6 nm. The pore size distribution of adsorbent represent the size of uniform pores.

4. Conclusion

In this paper, the spherical form of commercial activated alumina with mesopores and narrow size distribution were studied to characterize the most physical properties such as crush strength, particle size distribution, chemical and elemental analysis, adsorption isotherms etc. With the aid of modern devices like Tristar II micromeritics, three commonly used models, the Langmuir, Freundlich and BET equations were employed to correlate the experimental data. Results showed that BET model was fitted quite well with R-value more than 0.99 and it was selected as the most appropriate adsorption isotherm correlation. Using this model, the surface area and molecular cross-sectional area of HYAA300 were determined 334.6737 m^2/g and 0.162 nm^2, respectively. By comparison hysteresis loops of the adsorption-desorption of adsorbent with IUPAC was deduced that mesopore geometries of HYAA300 are tubular capillary that they had various forms of cross sections with open at both ends. The XRF analysis demonstrated that presence of more γ-alumina in composition was caused to increase strong crystalline structure while decreasing of the mineralogical inhomogeneity and intensity of activated alumina by acid activation method can be resulted in higher BET surface area and total pore volume. As

briefly, the specific surface area, pore mean diameter and pore volume of the activated alumina (HYAA300) were determined 334.67 m^2/g, 8.096 nm, and 0.0713 cm^3/g, respectively.

Acknowledgment

We would like to express our great appreciation to Mr. M.A. Fatemi for his valuable and constructive suggestion during the planning and development of this research work. Also the Nitel Pars Company (subsidiary of Fateh Group) and Hengye Molecular Sieve Company for their technical assistances gratefully acknowledged.

References

[1] H.C. Stumpf, A.S. Russell, J.W. Newsome, C.M. Tucker, Thermal Transformations of Aluminas and Alumina Hydrates - Reaction with 44% Technical Acid, Industrial & Engineering Chemistry, 42 (1950) 1398-1403.

[2] B.C. Lippens, Structure and texture of aluminas, in, Waltman, Delft, 1961.

[3] W.H. Gitzen, Alumina as a ceramic material, Columbus, Ohio : American Ceramic Society, 1970.

[4] K. Wefers, C. Misra, Oxides and hydroxides of aluminum, Alcoa Laboratories, [Estados Unidos], 1987.

[5] Z. Shi, W. Jiao, L. Chen, P. Wu, Y. Wang, M. He, Clean synthesis of hierarchically structured boehmite and γ-alumina with a flower-like morphology, Microporous and Mesoporous Materials, 224 (2016) 253-261.

[6] A.P. Borosy, B. Silvi, M. Allavena, P. Nortier, Structure and Bonding of Bulk and Surface .theta.-Alumina from Periodic Hartree-Fock Calculations, The Journal of Physical Chemistry, 98 (1994) 13189-13194.

[7] P. Euzen, P. Raybaud, X. Krokidis, H. Toulhoat, J.-L. Le Loarer, J.-P. Jolivet, C. Froidefond, Alumina, in: Handbook of Porous Solids, Wiley-VCH Verlag GmbH, 2002, pp. 1591-1677.

[8] R. Amrousse, Deposition of activated alumina powder on SiC diesel particulate filters with wall flow type through in-situ hydrothermal process, Powder Technology, 286 (2015) 557-560.

[9] W. El-Nadjar, M. Bonne, E. Trela, L. Rouleau, A. Mino, S. Hocine, E. Payen, C. Lancelot, C. Lamonier, P. Blanchard, X. Courtois, F. Can, D. Duprez, S. Royer, Infrared investigation on surface properties of alumina obtained using recent templating routes, Microporous and Mesoporous Materials, 158 (2012) 88-98.

[10] P.A. Nikulshin, P.P. Minaev, A.V. Mozhaev, K.I. Maslakov, M.S. Kulikova, A.A. Pimerzin, Investigation of co-effect of 12-tungstophosphoric heteropolyacid, nickel citrate and carbon-coated alumina in preparation of NiW catalysts for HDS, HYD and HDN reactions, Applied Catalysis B: Environmental, 176–177 (2015) 374-384.

[11] L.A. O'Dell, S.L.P. Savin, A.V. Chadwick, M.E. Smith, A 27Al MAS NMR study of a sol–gel produced alumina: Identification of the NMR parameters of the θ-Al2O3 transition alumina phase, Solid State Nuclear Magnetic Resonance, 31 (2007) 169-173.

[12] M. Takbiri, K.J. Jozani, A.M. Rashidi, H.R. Bozorgzadeh, Preparation of nanostructured activated alumina and hybrid alumina–silica by chemical precipitation for natural gas dehydration, Microporous and Mesoporous Materials, 182 (2013) 117-121.

[13] S.A. Yashnik, S.P. Denisov, N.M. Danchenko, Z.R. Ismagilov, Synergetic effect of Pd addition on catalytic behavior of monolithic platinum–manganese–alumina catalysts for diesel vehicle emission control, Applied Catalysis B: Environmental, 185 (2016) 322-336.

[14] A.R. Ferreira, E. Küçükbenli, S. de Gironcoli, W.F. Souza, S.S.X. Chiaro, E. Konstantinova, A.A. Leitão, Structural models of activated γ-alumina surfaces revisited: Thermodynamics, NMR and IR spectroscopies from ab initio calculations, Chemical Physics, 423 (2013) 62-72.

[15] Mónica Benítez-Guerrero, Luís A. Pérez-Maqueda, Pedro E. Sánchez-Jiménez, José Pascual Cosp, Characterization of thermally stable gamma alumina fibres biomimicking sisal, Microporous and Mesoporous Materials, 185 (2014) 167–178.

[16] C. Lesaint, G. Kleppa, D. Arla, W.R. Glomm, G. Øye, Synthesis and characterization of mesoporous alumina materials with large pore size prepared by a double hydrolysis route, Microporous and Mesoporous Materials, 119 (2009) 245-251.

[17] Q. Wu, F. Zhang, J. Yang, Q. Li, B. Tu, D. Zhao, Synthesis of ordered mesoporous alumina with large pore sizes and hierarchical structure, Microporous and Mesoporous Materials, 143 (2011) 406-412.

[18] Z.-Y. Yuan, B.-L. Su, Insights into hierarchically meso-macroporous structured materials, Journal of Materials Chemistry, 16 (2006) 663-677.

[19] A. Stanislaus, K. Al-Dolama, M. Absi-Halabi, Preparation of a large pore alumina-based HDM catalyst by hydrothermal treatment and studies on pore enlargement mechanism, Journal of Molecular Catalysis A: Chemical, 181 (2002) 33-39.

[20] Z. Wu, Q. Li, D. Feng, P.A. Webley, D. Zhao, Ordered mesoporous crystalline γ-Al2O3 with variable architecture and porosity from a single hard template, Journal of the American Chemical Society, 132 (2010) 12042-12050.

[21] F.-S. Shiau, T.-T. Fang, Low-temperature synthesis of α-alumina using citrate process with α-alumina seeding, Materials Chemistry and Physics, 60 (1999) 91-94.

[22] Q. Liu, A. Wang, X. Wang, P. Gao, X. Wang, T. Zhang, Synthesis, characterization and catalytic applications of mesoporous γ-alumina from boehmite sol, Microporous and Mesoporous Materials, 111 (2008) 323-333.

[23] M. Inoue, K. Kitamura, T. Inui, Synthesis of wide-pore alumina support from gibbsite, Journal of Chemical Technology & Biotechnology, 46 (1989) 233-247.

[24] N. Salahudeen, A.S. Ahmed, A.a.H. Al-Muhtaseb, M. Dauda, S.M. Waziri, B.Y. Jibril, J. Al-Sabahi, Synthesis, characterization and adsorption study of nano-sized activated alumina synthesized from kaolin using novel method, Powder Technology, 280 (2015) 266-272.

[25] S. Azarfar, S. Mirian, H. Anisi, R. Soleymani, S. Sadighi, Characterization of 3A molecular sieve using Tristar micromeritics device, in: The first conference on the new laboratory techniques in oil,gas and petrochemical industries, Tehran, 2015.

[26] I. Langmuir, The adsorption of gases on plane surfaces of glass, mica and platinum, J. Am. Chem. Soc, 40 (1918) 1361–1403.

[27] H. Freundlich, W. Heller, The Adsorption of cis- and trans-Azobenzene, J. Am. Chem. Soc, 61 (1939) 2228–2230.

[28] S. Brunauer, P.H. Emmett, E. Teller, Adsorption of Gases in Multimolecular Layers, Journal of the American Chemical Society, 60 (1938) 309-319.